

## **NASCAP-2K – AN OVERVIEW**

**M. J. Mandell**

Science Applications International Corporation  
10260 Campus Point Dr., M.S. A1, San Diego, CA, 92121  
Phone: 858-826-1622  
Fax: 858-826-1652  
E-mail: [myron.j.mandell@saic.com](mailto:myron.j.mandell@saic.com)

**V. A. Davis**

**B.M. Gardner**

**I. G. Mikellides**

Science Applications International Corporation

**D. L. Cooke**

Air Force Research Laboratory/VSBS

**J. Minor**

NASA Marshall Space Flight Center

### **Abstract**

Nascap-2k is the modern replacement for the older 3-D charging codes NASCAP/GEO, NASCAP/LEO, POLAR, and DynaPAC. Built on the DynaPAC kernel and incorporating surface charging, environment and space potential models from the older codes, Nascap-2k performs charging calculations for a wide variety of space environments under control of a unified graphical interface.

In this paper we illustrate the use of Nascap-2k for spacecraft charging calculations. We touch on some of the unique physical and mathematical models on which the code is based. Examples/demos include the use of Object Toolkit, charging calculations in geosynchronous substorm, solar wind, low earth orbit, and auroral environments, and display and analysis of surface potentials, space potentials and particle trajectories.

### **Introduction**

The recently released version 2.0 of Nascap-2k builds on the physical principles, mathematical treatments, computational algorithms, and user experience developed during over two decades of spacecraft charging research. Using Nascap-2k's graphical user interface (GUI) a scientist or engineer with minimal knowledge of spacecraft charging can easily set up, run, and analyze standard problem types in geosynchronous, low-earth-orbit, auroral, and solar wind environments. A more adventurous user can, within the Nascap-2k framework, go beyond the standard problem types to investigate novel or specialized spacecraft environment interactions.

Nascap-2k presents three GUIs to the user. The main Nascap-2k GUI is concerned with environment specification, calculation strategy, and results display and analysis. Object Toolkit

(OTk) is used to build spacecraft surface models for Nascap-2k analysis (as well as for analysis by other codes). GridTool is used to build nested cubic grids about the spacecraft model for calculation of electrostatic potentials and particle trajectories in the external space. In addition to these, the SEE Spacecraft Charging Handbook is an extremely useful companion application to Nascap-2k.

Beneath the Nascap-2k GUI are the calculation engines written in Fortran and C++. The potential solver (for potentials in the external space) and particle tracker (for charge densities, visualization, and PIC capabilities) are of DynaPAC (Mandell *et al.*, 1992) heritage. New is the BEM (Boundary Element Method, Brebbia 1981) module (written in C++) which incorporates the BEM charging algorithms (Mandell *et al.*, 2001), together with environment and surface charging physics treatments inherited from NASCAP/GEO (Katz *et al.*, 1977), NASCAP/LEO (Mandell and Davis, 1990), and POLAR. The BEM module also serves as the main line of communication between the Nascap-2k GUI and the detailed information stored in the Nascap-2k database (also of DynaPAC heritage).

Among the virtues of Nascap-2k is that electric fields in space are strictly continuous. This is done by expanding the space of the interpolation functions so that the electric field (as well as the potential) is defined at each node. Figure 1 compares trajectories of particles passing over a slab computed using trilinear interpolation and using Nascap-2k's approach. In Figure 1a, the result of a code using the standard trilinear interpolation, the trajectories are split by the grid points, clearly an artifact due to inadequate representation of electric fields in this trilinear code. Figure 1b shows the same calculation, done with the continuous field treatment. The particle deflection varies continuously (albeit non-monotonically) with position.

### **Object Toolkit (OTk)**

Object Toolkit was initially written to define spacecraft surface models for Nascap-2k. The reason for writing a new geometry engine was to avoid dependence on third-party software, which has proven to be expensive, difficult to learn, and awkward to adapt to our specific needs. OTk is customizable for use with other applications via an external file. To date, OTk has been customized for use with EPIC (Electric Propulsion Interactions Code) and at least one other code. OTk is written in pure Java, so that it is portable to any platform that supports a full Java implementation.

Figure 2a shows a solar array truss displayed in OTk. The truss was defined in OTk by manipulating and editing primitive "BOOM" objects. Such an object might also be defined by a standard finite element preprocessor (*e.g.* Patran) and imported into OTk.

Figure 2b shows the truss attached to a solar panel to form a "Wing." Note that the model was designed such that the nodes on the truss and panel matched precisely. When this happens, OTk automatically deletes the abutting surface elements.

The spacecraft body was defined as a "Box" primitive to which two "Panel" primitives were attached as radiators, and some editing was done to achieve the desired distribution of materials. Figure 2c shows the "Wing" attached to the spacecraft body. This common type of attachment is done by a "Wizard", which automatically orients the two parts, positions them, and edits the

mesh to be fully “compatible.” Less common attachments can be done by performing the individual operations “manually” via menu choices and dialogs. The final model (body with two “Wings”) is shown in Figure 2d. In subsequent sections, we will show charging calculations for this model in geosynchronous, interplanetary, and auroral environments. We will show charging of a different model in LEO environment.

OTk contains a default selection of common spacecraft materials. Properties of these materials govern secondary emission, conductivity, etc. The properties can be edited, and new materials can be added and assigned properties. The SEE Program provides a library of additional materials with well-documented, recently measured properties in a format that can be easily imported into Otk.

### **Geosynchronous Charging**

To perform a simulation of charging at geosynchronous altitudes, we use the Nascap-2k GUI to define a plasma environment (Maxwellian or Double Maxwellian), sun direction and intensity, and a timestepping strategy. Initial surface potentials and/or conductor bias can be defined as appropriate. Since the Boundary Element Method is used for surface charging, external gridding is not required. However, if the external potentials and electric field and/or particle trajectories are of interest, GridTool is used to appropriately grid the external space in preparation for such calculations.

Figure 3 shows the result of a calculation of geosynchronous charging in sunlight, using the “NASA Worst Case” plasma environment (Purvis *et al.*, 1984), displayed in the Nascap-2k GUI. The maximum differential charging occurs toward the outboard end of the solar array, and the saddle point potential structure can be seen. Detailed results for selected surface elements can be shown in popup windows, and we can also readily obtain the time histories of potentials and currents to individual cells or groups of cells.

### **Solar Wind (Interplanetary) Charging**

A spacecraft outside Earth’s magnetosphere is exposed to an interplanetary environment that consists of solar UV radiation and the solar wind plasma. The approximate mean parameters of the solar wind plasma (Vilas *et al.*, 1988) at 1 AU are shown in Table 1. The plasma currents are well below the solar-induced photoelectron currents (above  $10^{-5}$  Am<sup>-2</sup> for most materials). Therefore, illuminated surfaces tend to charge to positive potentials (often tens of volts) to the point where the attenuated photoemission matches the enhanced collection of plasma electrons. To model this charging requires a model of the photoemission electron spectrum, which falls off much more slowly in the range of tens of volts than it does in the range of a few volts.

Figure 4ab shows an example of a charging calculation in an interplanetary environment. The solar cells maintain, on average, a positive potential of order 15 volts. As the dark insulators gradually charge, bootstrap charging takes over and takes the spacecraft negative. Note that the time-history post-processing facility can present both potentials and currents for groups of cells or individual cells, and the plotted results can be retrieved as text for pasting into a spreadsheet or other program for further analysis.

**Table 1. Approximate average solar wind parameters at 1 AU.**

Plasma Density	$7 \times 10^6 \text{ m}^{-3}$
Proton Velocity	$430 \text{ km s}^{-1}$
Proton Energy	1 keV
Proton Current	$5 \times 10^{-7} \text{ A m}^{-2}$
Electron Temperature	15 eV
Electron Thermal Current	$7 \times 10^{-7} \text{ A m}^{-2}$

### **Auroral Charging**

Spacecraft passing through auroral arcs, especially at night during dropouts of cold plasma, have been observed to charge to potentials of a kilovolt or more. (Gussenhoven *et al.*, 1985.) Figure 5a shows the Nascap-2k definition of an auroral environment in Fontheim (Fontheim *et al.*, 1982) form. In addition to the cold plasma environment, energetic electrons are divided into Gaussian, Maxwellian, and power law components. The SEE Spacecraft Charging Handbook (Katz *et al.*, 2001) provides two once-observed examples of such environments. From the complexity of this environment, it seems clear that further research is needed to provide guidelines as to how the auroral environment should best be represented for the purpose of charging analysis.

Figure 5b shows time-dependent charging of our model spacecraft in this environment. After about one second, the model has developed about 150 volts of overall charging and over 100 volts of differential charging; both types of charging are continuing to increase, albeit at a lesser rate.

Figure 5c shows a display of ion trajectories superimposed on surface and space potentials. These trajectories were specified to originate on a potential contour in a plane near the potential cutplane. The plot shows that ram ions entering this contour that do not impact the ramward side of the solar array eventually strike the rear of the charged spacecraft, slowing the charging process.

### **Low-Earth Orbit Charging**

The cold, dense plasma that prevails in low-Earth orbit is a fairly benign environment for most purposes. However, applied high voltages (Mandell and Katz, 1990), a significant magnetic field, ram-wake effects, and sensitive scientific instruments can lead to interesting calculations. As an example, we consider the charging of an octagonal satellite whose three ram-facing facets consist of conductive experiment plates and ITO coated solar cells, and the remaining five facets (zenith, nadir, and three wake facets) are covered with uncoated cells or other insulators. The ends are also conductive. The environment is a plasma with density  $3 \times 10^{11} \text{ m}^{-3}$  and temperature of 0.15 eV. The magnetic field is 0.25 gauss northward (parallel to the long axis) and 0.25 gauss vertical.

Figure 6abc shows the results of the calculation after 0.5 seconds. The vertical component of the magnetic field induces an end-to-end potential of nearly one volt, with the positive end at about -0.2 volts and the negative end at about -0.9 volts. The nadir and zenith insulating surfaces are in equilibrium at about -0.75 volts, while the wake surfaces have reached about -1.3 volts and continue to charge slowly. (The wake surface potentials are limited by photoemission when in sunlight, or by bulk conductivity of the coverglasses.) The wake structure behind the spacecraft is clearly shown by both potential contours and ion trajectories in Figure 6a.

Of interest is the current balance to the spacecraft. Electrons are collected predominantly on the southern (less negative) conducting end (conductor 3 in Figure 6c), and on the nearby ram facing surfaces. The conductive ram-facing surfaces (conductor 1 in Figure 6c) primarily collect ram ions. Thus, a parasitic plasma current of about 0.4 mA flows through the spacecraft from negative to positive (as in a battery), with the negative terminal distributed over the ram-facing surfaces, and the positive terminal located primarily on the southern end of the spacecraft. Reversing the sign of the vertical component of magnetic field moves the positive terminal to the northern end.

### **Summary**

Nascap-2k is a modern computer code that simulates spacecraft charging in a variety of environments. Among the modern features of Nascap-2k are use of the Boundary Element Method (BEM) for surface charging, and space potentials with strictly continuous electric fields.

This paper outlined the definition of a simple spacecraft model using Object Toolkit, and showed results of charging calculations for that model in Geosynchronous, Auroral, and Interplanetary environments. A different spacecraft model was used to show magnetic field and wake effects for a low-Earth orbiting satellite. These calculations can be done in Nascap-2k with both a relative ease and a high degree of flexibility. In addition, several different types of diagnostics are provided to study and understand the results.

For additional information or to obtain *Nascap-2K*, contact Jody Minor, [jody.minor@nasa.gov](mailto:jody.minor@nasa.gov).

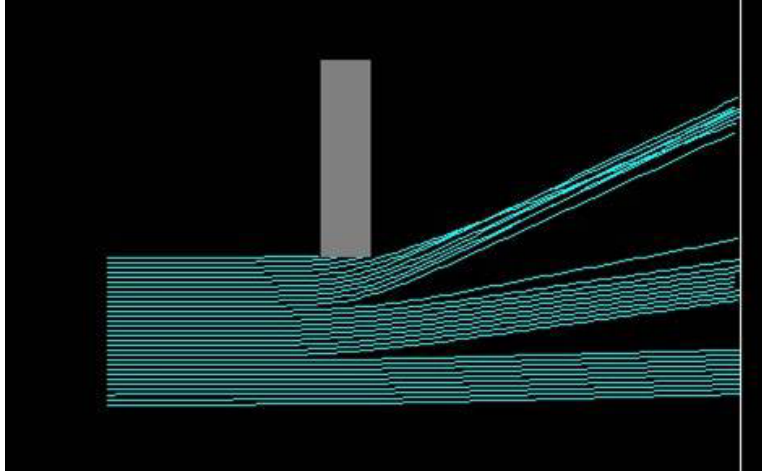


**Figure 1a. Particle trajectories over a charged slab using a code with trilinear potential interpolation.**

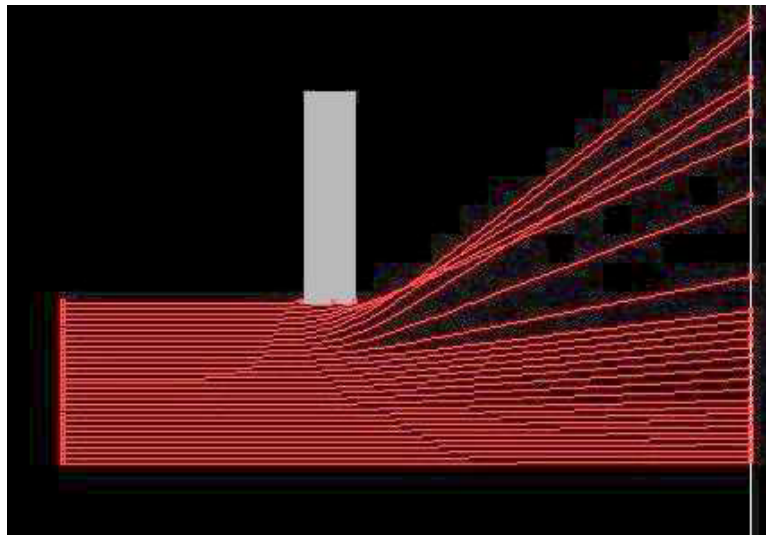


**Figure 1b. Particle trajectories over a charged slab calculated using Nascap-2k with continuous electric fields.**

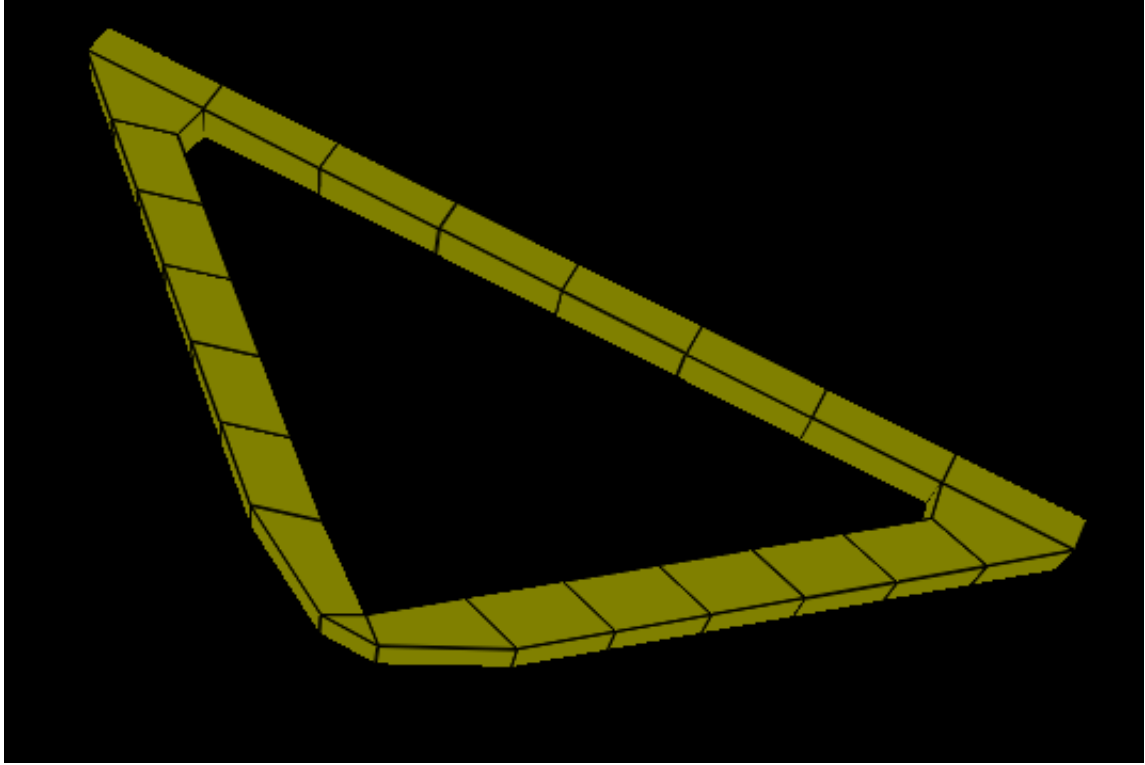


**Figure 2a. Object Toolkit model of truss for mounting solar array.**

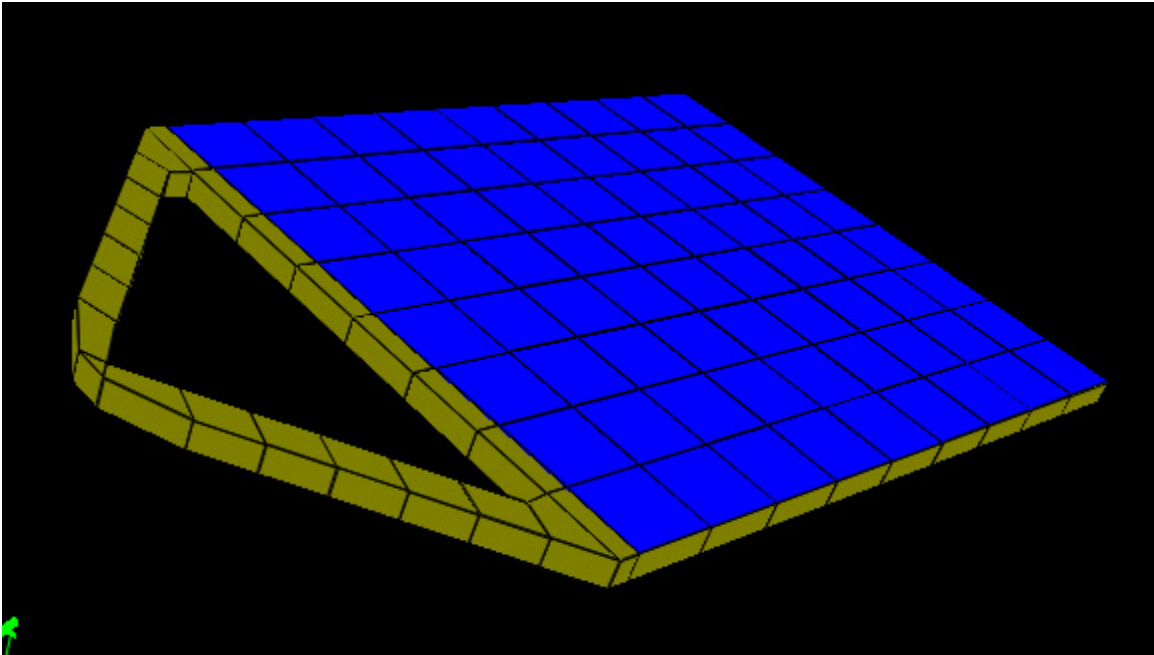


**Figure 2b. Object Toolkit model of solar array wing.**

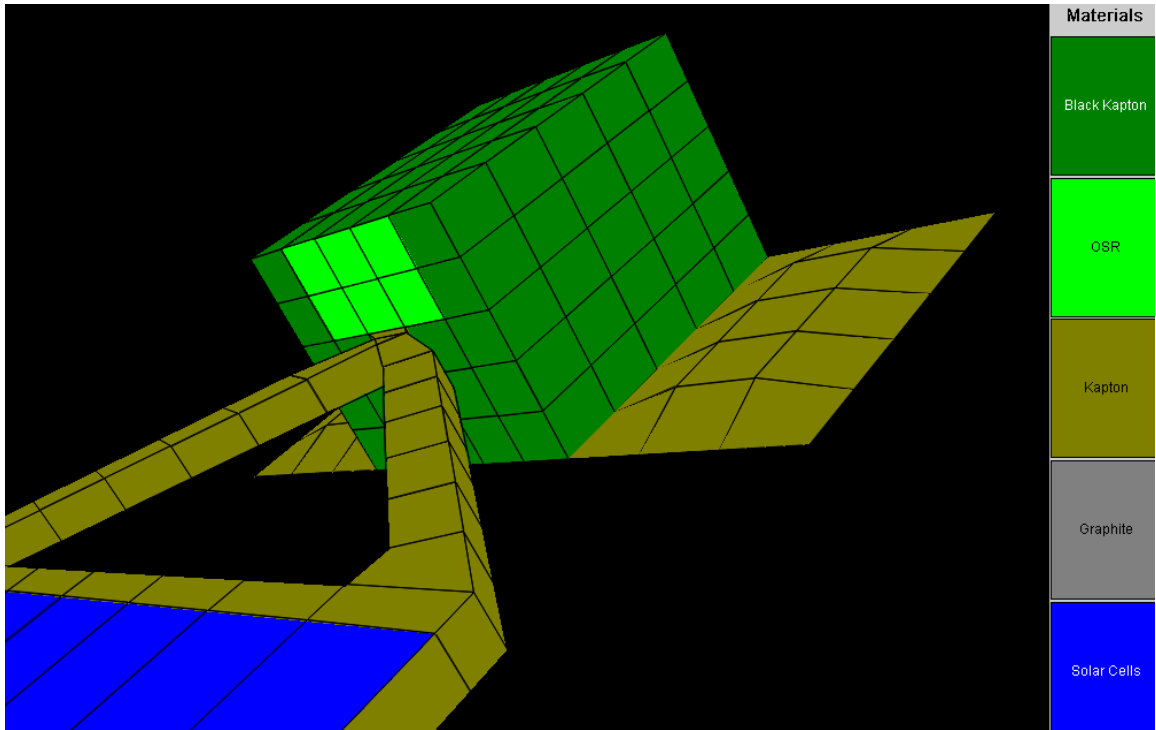


**Figure 2c. Object ToolKit model of spacecraft body with wing attached.**

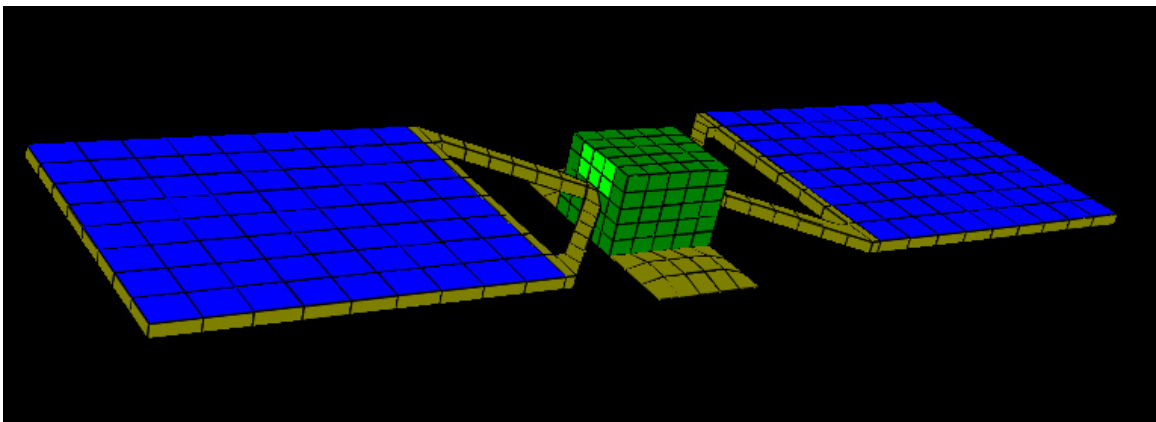


**Figure 2d. Object Toolkit model of spacecraft.**

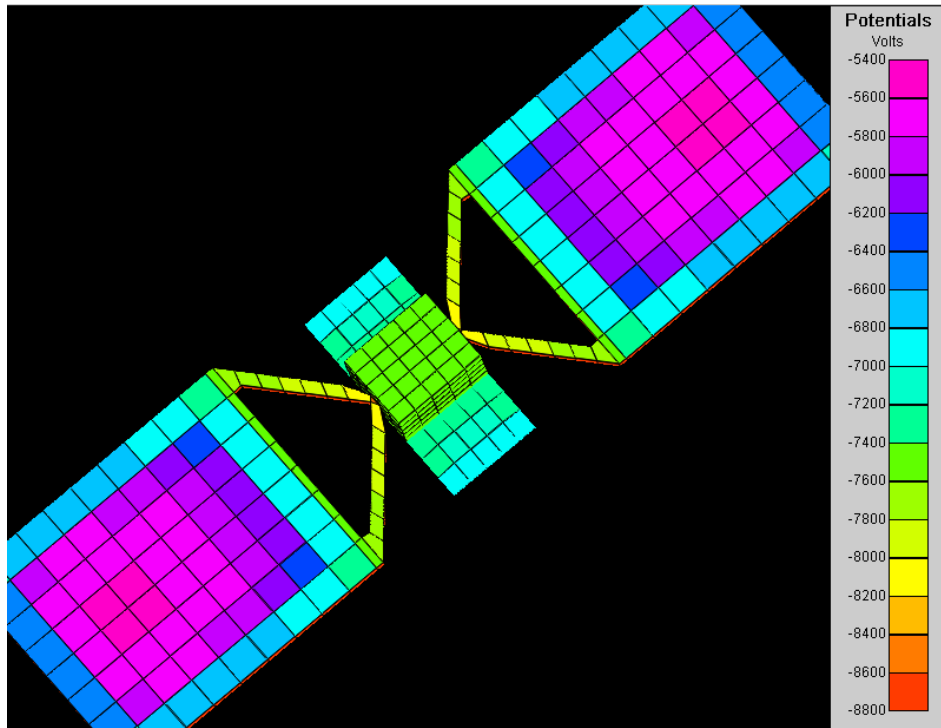


**Figure 3a. Geosynchronous charging result, showing maximum differential charging toward outboard end of solar panels.**

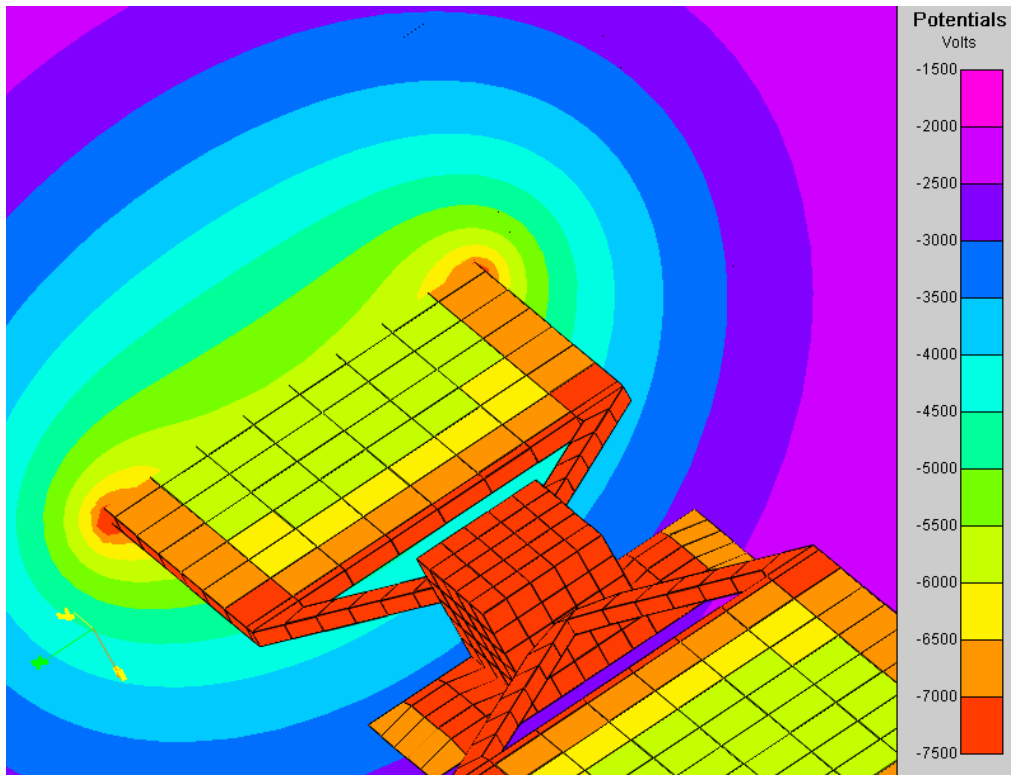


**Figure 3b. Geosynchronous charging result, showing saddle point over solar panel.**

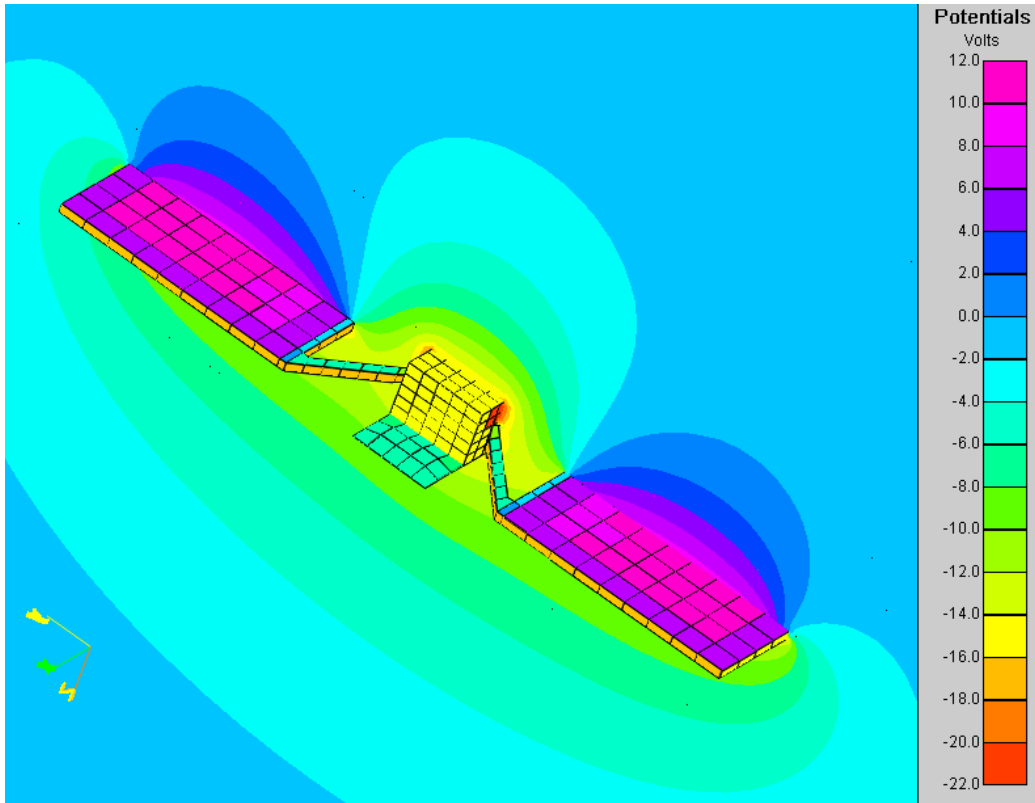


**Figure 4a. Potentials calculated for spacecraft in solar wind environment.**

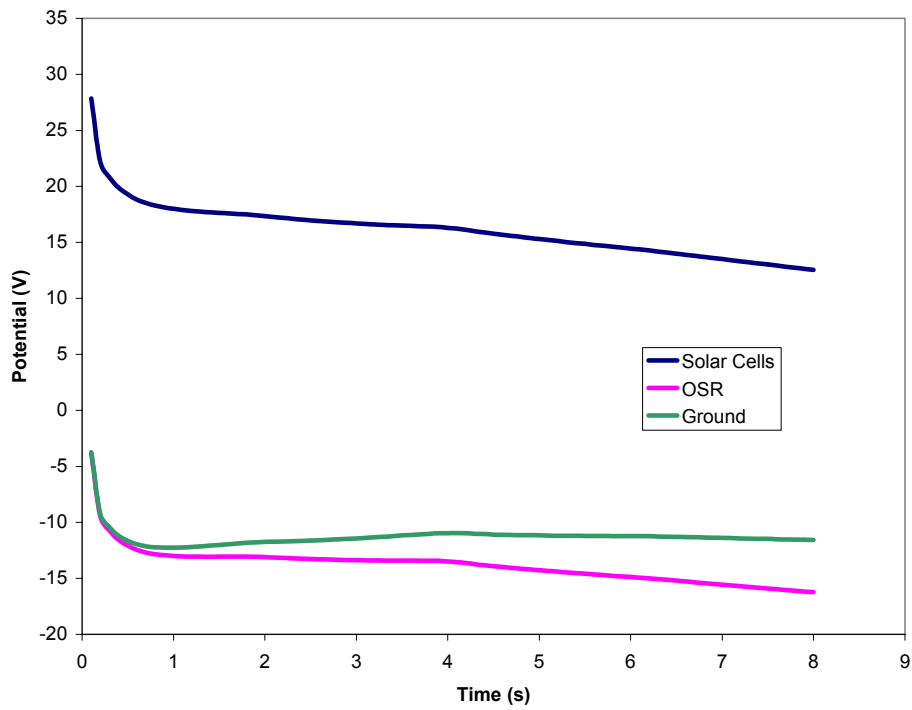


**Figure 4b. Time history of potentials for solar wind calculation.**

### Polar Environment

#### Auroral Environment Plasma

##### Low Energy

Density ( $m^{-3}$ ): 3.550E9

Temperature (eV): 0.200

Debye Length (m): 5.580E-2

E. Current ( $Am^{-2}$ ): 4.256E-5

Ion Current ( $Am^{-2}$ ): 2.492E-7

##### Maxwellian

E. Current( $Am^{-2}$ ): 1.400E-6

Temperature (eV): 8000.

Density ( $m^{-3}$ ): 5.808E5

Coefficient: 4.346E4

##### Gaussian

E. Current( $Am^{-2}$ ): 1.400E-5

Energy (eV): 2.400E4

Width (eV): 1.600E4

Density ( $m^{-3}$ ): 7.770E6

Coefficient: 4.075E4

##### Power Law

E. Current( $Am^{-2}$ ): 6.700E-7

1st Energy (eV): 50.00

2nd Energy (eV): 1.600E6

Exponent: 1.100

Density ( $m^{-3}$ ): 1.034E6

Coefficient: 3.049E11

#### Sun

Sun Direction

X: 0.0    Y: 0.0    Z: -1.000

Relative\* Sun Intensity: 0.0

\*(value at Spacecraft) / (value at Earth Orbit)

#### Magnetic Field (T)

Bx: 0.0    By: 0.0    Bz: 0.0

#### Spacecraft Velocity (m/s)

Vx: 0.0    Vy: 0.0    Vz: -7500.

#### Particle Species

Type	Mass (amu)	Charge (C)	%
Electron	5.486E-4	-1.602E-19	100.0
Oxygen	16.00	1.602E-19	100.0
HYDROGEN	1.000	1.602E-19	0.0

**Figure 5a.** Example of auroral environment, as used in sample auroral charging calculation.

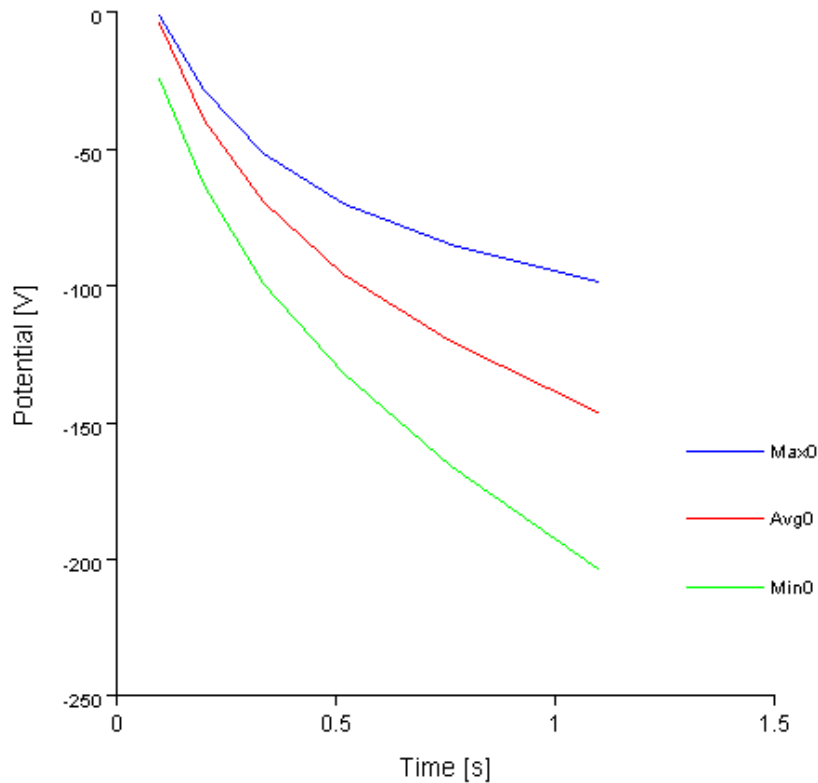


**Figure 5b.** Time dependence of overall and differential charging for the sample auroral charging calculation.

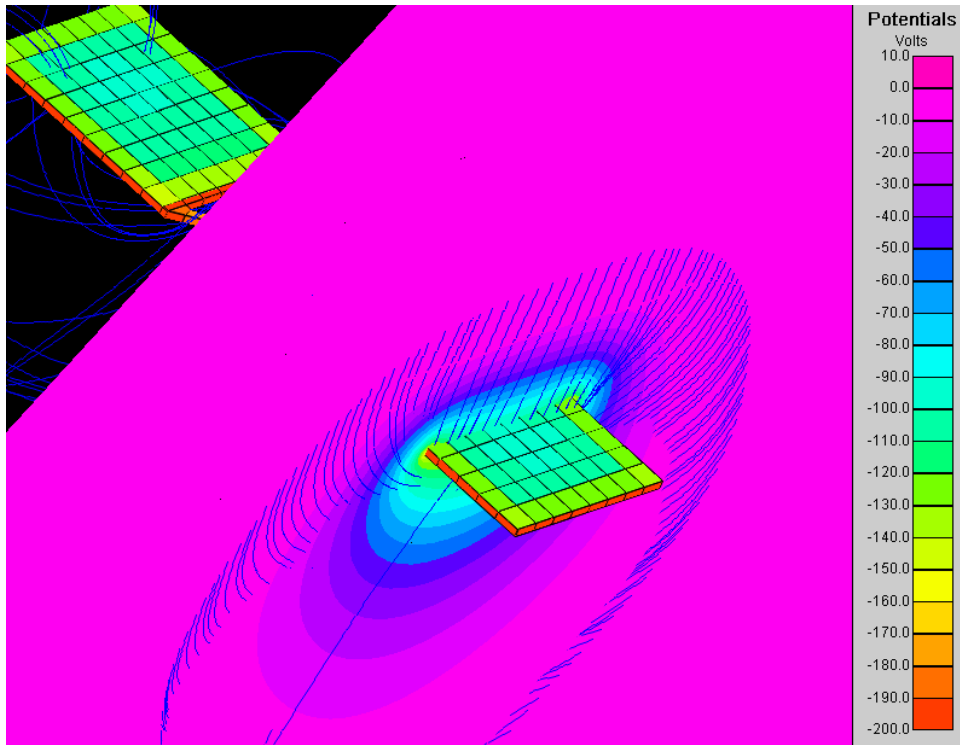


**Figure 5c. Surface potentials, space potentials, and particle trajectories for the auroral charging example.**

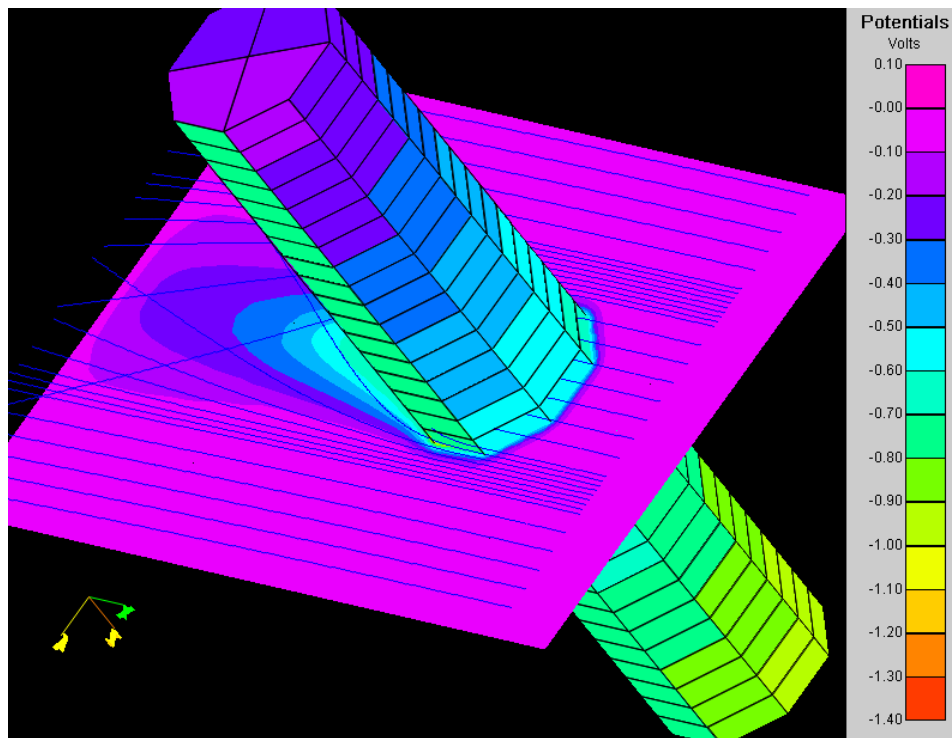


**Figure 6a. Charging and wake structure of an octagonal satellite in low-Earth orbit. (See text for details.)**

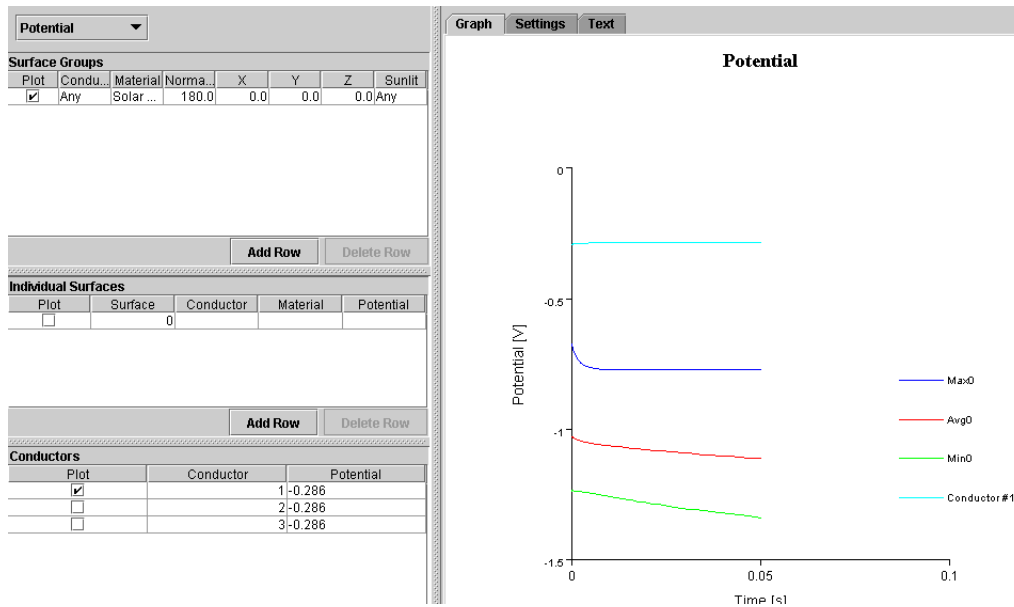


**Figure 6b. Surface potentials for the octagonal satellite. The upper line represents the ground potential (to which  $v \times B$  variation must be added). Second line is for nadir and zenith solar cells, and bottom line is for wake-facing solar cells.**

Conductors		
Plot	Conductor	Charging Current
<input checked="" type="checkbox"/>	1	4.127E-4
<input checked="" type="checkbox"/>	2	5.522E-6
<input checked="" type="checkbox"/>	3	-3.912E-4

**Figure 6c. Current collected by the ram-facing conducting cells (top), negative-end conducting cells (middle), and positive-end conducting cells (bottom).**

## References

1. S.A. Brebbia, Boundary Element Methods, Springer Verlag, New York, 1981.
2. E.G. Fontheim, K. Stasiewicz, M. O. Chandler, R. S. B. Ong, "Statistical Study of Precipitating Electrons, Journal of Geophysical Research 87, 3469, 1982.
3. M.S. Gussenhoven, D. A. Hardy, F. Rich, W. J. Burke, H.-C. Yeh, "High-Level Spacecraft Charging in the Low-Altitude Polar Auroral Environment", Journal of Geophysical Research 90, 11009, 1985.
4. I. Katz, D. E. Parks, M. J. Mandell, J. M. Harvey, D. H. Brownell, S. S. Wang, and M. Rotenberg, A Three Dimensional Dynamic Study of Electrostatic Charging in Materials, NASA Rep. CR-135256, August 1977.
5. I. Katz, V. A. Davis, M. J. Mandell, B. M. Gardner, J. M. Hilton, A. R. Fredrickson, D. L. Cooke, J. Minor, "Spacecraft Charging Interactive Handbook," 7<sup>th</sup> Spacecraft Charging Technology Conference, Noordwijk, The Netherlands, 23-27 April 2001.
6. M.J. Mandell and I. Katz, "High Voltage Plasma Interactions Calculations Using NASCAP/LEO", AIAA Paper AIAA-90-0725, 1990.
7. M.J. Mandell and V. A. Davis, User's Guide to NASCAP/LEO, 1990.
8. M.J. Mandell, T. Luu, J. Lilley, G. Jongeward, and I. Katz, Analysis of Dynamical Plasma Interactions with High Voltage Spacecraft, (2 volumes), Rep. PL-TR-92-2258, Phillips Lab., Hanscom Air Force Base, MA, June 1992.
9. M.J. Mandell, I. Katz, J. M. Hilton, D. L. Cooke, J. Minor, "Nascap-2K Spacecraft Charging Models: Algorithms and Applications," 7<sup>th</sup> Spacecraft Charging Technology Conference, Noordwijk, The Netherlands, 23-27 April 2001.
10. C.K. Purvis, H.B. Garrett, A.C. Whittlesey, and N.J. Stevens, Design Guidelines for Assessing and Controlling Spacecraft Charging Effects, NASA TP 2361, 1984.
11. F. Vilas, C. R. Chapman, M. S. Matthews (editors), MERCURY, Tucson: University of Arizona Press, 1988.